Available online at www.sciencedirect.com
ScienceDirect
International Journal of Heat and Mass Transfer 50 (2007) 1706–1714
International Journal of HEAT and MASS TRANSFER
www.elsevier.com/locate/ijhmt

Multi-parameter estimation in combined conduction–radiation from a plane parallel participating medium using genetic algorithms

Swati Verma, C. Balaji *

Heat Transfer and Thermal Power Laboratory, Department of Mechanical Engineering, Indian Institute of Technology, Chennai 600 036, India

Received 24 May 2004; received in revised form 15 October 2006
Available online 29 December 2006

Abstract

An inverse conduction–radiation problem for simultaneous estimation of the conduction–radiation parameter, the optical thickness and the boundary emissivity from a knowledge of the measured temperature profile for combined conduction and radiation in a plane parallel participating medium is presented. A finite volume method is used to solve the "forward" problem, wherein the temperature profile is determined by a solution of the governing equation for a given set of parameters. The inverse problem is treated as an optimization problem, wherein, we minimize the sum of square of residuals between the measured and estimated temperatures. Genetic algorithms are used for the search. The effects of "measurement" errors on the estimated parameters, which are introduced through a random perturbation, are investigated.

Keywords: Conduction–radiation parameter; Plane parallel participating medium; Finite volume method; Inverse problem; Genetic algorithms

1. Introduction

Inverse problems in a participating medium are important in the field of heat transfer. Inverse analyses provide a great advantage where direct measurement of desired quantities is not possible for several reasons. Inverse combined conduction–radiation problems are important in fibrous insulation, glass manufacture and in many other applications. General inverse combined conduction–radiation problems in a participating medium deal with the estimation of optical thickness and conduction–radiation parameter. Li [1] presented results for an inverse conduction–radiation problem wherein a simultaneous estimation of single scattering albedo, the optical thickness, the conduction–radiation parameter and the scattering phase function from a knowledge of exit radiation intensities was carried out. The problem was solved by using the conjugate gradient method to minimize the error between the calculated exit intensities and the experimental data. Manickavasagam and Menguc [2] employed the Levenberg–Marquardt method to estimate the optical thickness and radiation–conduction parameter of a one-dimensional plane parallel medium from the input temperature data measured inside the medium. Ruperti et al. [3] studied the inverse problem for estimating surface temperatures and fluxes from simulated temperatures measured within a semitransparent slab. A space marching technique was adopted to solve the inverse conduction–radiation problem.

Genetic algorithms (GA) are new to thermal engineering problems. The probability of finding the global optimum using GA is expected to be high for inverse problems. Genetic algorithms are computerized search and optimization algorithms based on the mechanics of natural selection. GA mimics the principle of survival of the fittest nature to make a search process. Li and Yang [4] solved an inverse radiation problem for the estimation of single scattering albedo, the optical thickness and the phase functions from the knowledge of the exit radiation intensities using GA. Kim, Baek and Ryou [5] presented an inverse

* Corresponding author. Tel.: +91 22 574689; fax: +91 22 570509.
E-mail address: balaji@iitm.ac.in (C. Balaji).

0017-9310/$ - see front matter © 2006 Elsevier Ltd. All rights reserved.
doi:10.1016/j.ijheatmasstransfer.2006.10.045

Nomenclature

A_s	surface area of the control volume, m^2
F, f	functions
I	radiation intensity, $W\,m^{-2}\,sr^{-1}$
k	thermal conductivity, $W\,m^{-1}\,K^{-1}$
L	distance between two parallel plates, m
$\vec{n}$	unit vector normal to d A_s
M	number of directions
N	number of control volumes
N_{CR}	conduction–radiation parameter, $k\kappa/4\sigma T_H^3$
q''	local heat flux, $W\,m^{-2}$
q^*	dimensionless heat flux for radiative equilibrium, $q''/\sigma(T_H^4 - T_C^4)$
R	residual temperature function or objective function, K^2
$\vec{s}$	unit vector along s direction
S	distance between interpolation point uf and integration point f, m
T	absolute temperature, K
z	z axis
Z	dimensionless length, z/L

Greek symbols

ε	hemispherical, total emissivity of the surface
γ	polar angle, radian
κ	absorption coefficient, m^{-1}
ω	solid angle, steradian (sr)
ϕ	azimuthal angle, radian
ψ_c	dimensionless conductive heat flux, $\frac{q''_c}{\sigma T_H^4}$
ψ_t	dimensionless total heat flux, $\frac{q''_c}{\sigma T_H^4} + \frac{q''_r}{\sigma T_H^4}$
σ	Stefan–Boltzmann constant, 5.67×10^{-8}, $W\,m^{-2}\,K^{-4}$
τ	dimensionless optical thickness, κL
τ_z	dimensionless optical thickness at any distance z, κz
θ	dimensionless temperature, T/T_H

Subscripts

a	average
b	black body
c	conductive
C	cold surface
n, s	north and south face of control volume
N, S	north and south nodes
f	integration point
H	hot surface
r	radiative
t	sum of conduction and radiation
uf	interpolation point

Superscript

l	corresponding to solid angle

analysis for estimating the wall emissivities for an absorbing emitting and scattering medium in a two-dimensional irregular geometry with diffusing emitting and reflecting opaque boundaries from the measured temperature. The finite volume method was used employed to solve the radiative transfer equation for a two-dimensional irregular geometry. A hybrid genetic algorithm that contains a local optimization algorithm was adopted to estimate wall emissivities by minimizing an objective function.

The inverse problem considered in this paper concerns the estimation of the conduction–radiation parameter, the optical thickness and boundary emissivity for a emitting and absorbing medium enclosed between two parallel, isothermal, infinitely long and diffuse plates. The inverse problem is formulated as the minimization of least square residual function between the measured and estimated temperature profiles and is solved by using GA.

2. Physical model

Fig. 1 shows the schematic of the geometry considered for the present study. The heated bottom wall is at a specified temperature T_H and the top wall is at T_C, and $T_H > T_C$. The numerical values of T_H and T_C in this study are 600 and 300 K, respectively. The walls are diffuse and gray and have the same emissivity ε. The medium enclosed

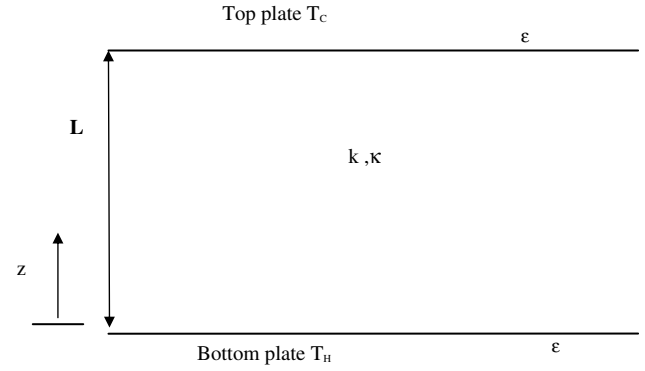

Fig. 1. Schematic of parallel plate enclosure with bottom wall heated and top wall cooled.

by the two parallel plates is absorbing, emitting but non-scattering, with uniform conduction and radiation properties. The medium is assumed to be gray and stationary, thereby tacitly implying that convection is ignored. Steady state conduction takes place in the enclosure. The one-dimensional medium is divided into N_z control volumes of length Δz in the z-direction, as shown in Fig. 2a. The solid angle of 4π is subdivided into conical solid angle elements (γ^-, γ^+) as shown in Fig. 2b. The direction, also an independent variable, is subdivided into M solid angles, where M represents the number of directions in the total

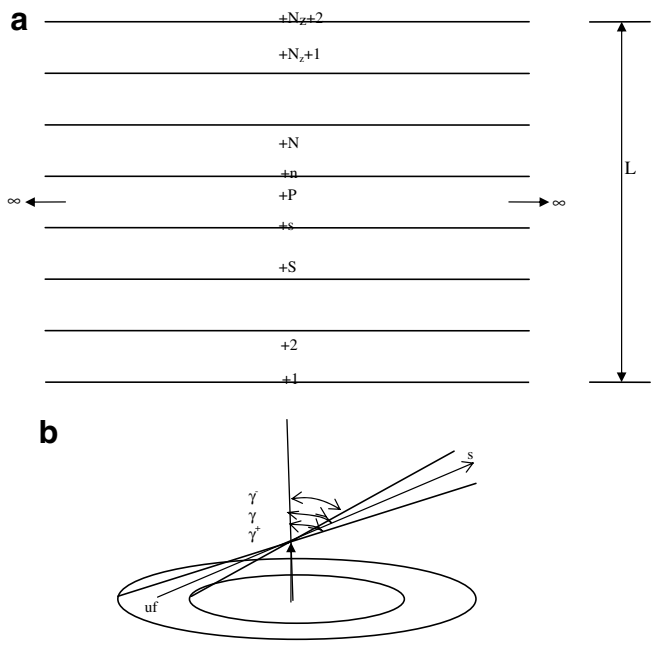

Fig. 2. (a) Typical control volume centered at node P along with neighboring nodes N and S. (b) Typical solid angles.

polar angle γ of π radians. In this case, because of symmetry, the intensity is a function of only z and γ, that is, for a given (z, γ), the intensity is same for all azimuthal angles ϕ from 0 to 2π.

3. Mathematical formulation

3.1. Forward problem

The equation governing the steady state temperature distribution in vectorial notation can be given by

$$k\nabla^2 T = \nabla \cdot q''_{\mathrm{r}}, \tag{1}$$

where the left-hand side represents the net conduction heat transfer into a differential control volume, the right-hand side gives the net radiation transfer leaving a differential control volume and k, T and q''_{r} represent the thermal conductivity, temperature and radiant heat flux, respectively. Integrating Eq. (1) over a typical control volume as shown in Fig. 2a

$$\int\int\int_v (k\nabla^2 T)\mathrm{d}v = \int\int\int_v \nabla \cdot q''_{\mathrm{r}}\mathrm{d}v, \tag{2}$$

Replacing ∇^2 operator by $\frac{\partial^2}{\partial z^2}$ and on application of the Gauss Divergence theorem to the right-hand side of Eq. (2), we get

$$\int\int_A k\frac{\partial^2 T}{\partial z^2}\mathrm{d}z = \int\int_{A_{\mathrm{s}}} q''_{\mathrm{r}} \cdot \vec{n}\mathrm{d}A_{\mathrm{s}}, \tag{3}$$

where $\vec{n}$ is the unit vector normal to the elemental surface area $\mathrm{d}A_{\mathrm{s}}$ and $\mathrm{d}v = 1.1.\mathrm{d}z = \mathrm{d}z$.

Expressing radiant heat flux in terms of intensity I in the direction of $\vec{s}$ contained in the elemental solid angle $\mathrm{d}\omega$, Eq. (3) becomes

$$\int\int_A k\frac{\partial^2 T}{\partial z^2}\mathrm{d}z = \int\int\int_{4\pi A_{\mathrm{s}}} I(\vec{s}\cdot\vec{n})\mathrm{d}A_{\mathrm{s}}\mathrm{d}\omega. \tag{4}$$

By applying the equation of radiation transfer, the right-hand side of Eq. (4) becomes

$$\int_{4\pi}\int\int_{A_{\mathrm{s}}} I(\vec{s}\cdot\vec{n})\mathrm{d}A_{\mathrm{s}}\mathrm{d}\omega = \int_{4\pi}\int\int_v [-\kappa I + \kappa I_{\mathrm{b}}]\mathrm{d}v\mathrm{d}\omega \tag{5}$$

$$= -4\pi\kappa I_{\mathrm{a}} v + 4\pi\kappa I_{\mathrm{b}} v, \tag{6}$$

where κ is the absorption coefficient. In addition,

$$I_{\mathrm{a}} = \frac{1}{4\pi}\sum_l I^l\omega^l \quad \text{is the average intensity,} \tag{7}$$

and $I_{\mathrm{b}} = \frac{n^2\sigma T^4}{\pi}$ is the average black body intensity corresponding to the temperature of the medium within the control volume and n is the refractive index of the semi transparent medium. The total solid angle of 4π is divided into a discrete number of solid angle elements and the average intensity in Eq. (7) is obtained as the weighted average of the intensity within the discrete solid angle elements ω^1.

Thus, Eq. (4) becomes

$$\int\int_A k\frac{\partial^2 T}{\partial z^2}\mathrm{d}z = -4\pi\kappa I_{\mathrm{a}} v + 4\pi\kappa I_{\mathrm{b}} v. \tag{8}$$

Dimensionless variables $\theta = \frac{T}{T_{\mathrm{H}}}$, $Z = \frac{z}{L}$ are introduced to convert Eq. (8) into a dimensionless form given by

$$\int\int_A \left(\frac{\partial^2\theta}{\partial Z^2}\right)\mathrm{d}Z = [\kappa L][4\sigma T_{\mathrm{H}}^3 L/k]\left[\theta^4 - \frac{\pi I_{\mathrm{a}}}{\sigma T_{\mathrm{H}}^4}\right]\Delta Z, \tag{9}$$

where T_{H} is the reference temperature, which in this case is the hot wall temperature and L is the characteristic length of the domain.

There are two unknowns in Eq. (9) namely temperature and intensity. Hence, another equation is required to solve the system of simultaneous equations, apart from the boundary conditions. The required equation, describing the change of intensity over a path length (The equation of radiation transfer, RTE) can be written as

$$\frac{\mathrm{d}I}{\mathrm{d}s} = -\kappa I + \kappa I_{\mathrm{b}}, \tag{10}$$

where the first term on the right-hand side is the attenuation through absorption and the second term is augmentation due to emission. In the case of gray medium approximation, the absorption coefficient. κ is a wavelength averaged quantity. The left-hand side represents the rate of change of intensity.

Integrating Eq. (10) over the control volume and ω^l and approximating all the variables on the right-hand side to be

constant at the nodal value while carrying out the volume integration, results in

$$\sum_{f=1}^{\text{no. of control panels}} A_{s,f}\int_{\omega^l} I_f(\vec{s}\cdot\vec{n}_f)\mathrm{d}\omega = [-\kappa I_P^l + \kappa I_{b,P}^l]v_P\omega^l, \tag{11}$$

where the surfaces of control volume are divided into f control panels. $A_{s,f}$ represents the surface area of each control panel and the intensity and the unit normal to the surface have been approximated as integration point f, which is the central point of the control volume.

The determination of I_f is similar to that proposed by Raithby and Chui [6]. The value of I_f is found by tracing back along the path taken by the ray in reaching f along the $-\vec{s}$ direction until a location is reached at which the intensity can be obtained by interpolation between nodal values. The interpolation point is designated as uf. Integration of Eq. (11) over a path length is performed to estimate the value of I_f in terms of I_{uf}. Hence

$$I_f = I_{uf}\mathrm{e}^{-\kappa_f s} + I_{b,f}(1-\mathrm{e}^{-\kappa_f^s}) - \frac{\left(\frac{\partial I_b}{\partial S}\right)_f}{\kappa_f}[1-\mathrm{e}^{-\kappa_f s}(1+\kappa_f S)] \tag{12}$$

Substitution of Eq. (12) into Eq. (11) results in the expression of heat transfer across all the control panels within ω^l in terms of I_{uf}, $I_{b,f}$. The value of $I_{b,f}$ is obtained by a linear interpolation using neighboring nodal values.

3.2. Inverse problem

In this study, the inverse analysis for the combined mode heat transfer in the geometry given for parameter estimation is carried out for three cases:

(a) The boundary property, i.e. emissivity ε of the walls (single parameter estimation),
(b) The thermal properties of medium, i.e. Conduction–radiation parameter N_{CR} and optical thickness τ (two parameter estimation), and
(c) Simultaneously thermal properties N_{CR} and τ and boundary property ε (three parameter estimation).

The parameters, to be estimated, are regarded as unknown while the measured temperature profile at a set of discrete points is available. The problem can be solved by minimization of objective function R which is expressed by the sum of square of residuals between estimated and measured temperatures, as shown below

$$R = \sum_{1}^{\text{no. of nodes}} [T_{\text{estimated}} - T_{\text{measured}}]^2 \tag{13}$$

where $T_{\text{estimated}}$ is the estimated temperature with the parameters (ε, N_{CR} and τ) and T_{measured} the "measured" temperature at each node. The minimization procedure is performed using genetic algorithms.

4. Solution procedure

4.1. Forward problem

For all the inner control volumes, the first derivative is approximated by second order accurate central difference expressions and on substitution in Eq. (9), the following equation is obtained.

$$\frac{(\theta_N+\theta_S-2\theta_P)}{\Delta Z} = [\kappa L]\left[\frac{4\sigma T_H^3}{k}\right]\left[\theta_P^4 - \frac{\pi I_a}{\sigma T_H^4}\right]\Delta Z \tag{14}$$

The above equation is valid for the inner control volumes. For the boundary control volumes, the walls happen to be one of the faces and hence the first order derivative is obtained using second order accurate forward or backward difference expressions.

Eq. (14) is non-linear in θ and is linearised by using the relation

$$\theta^4 = 4\theta_k^3\theta_{k+1} - 3\theta_k^4 \tag{15}$$

where k, $k+1$ denote, respectively, the old and new iterates. Linearization helps in reducing Eq. (14) to a set of linear equations, which may be solved easily.

Substituting Eq. (15) in Eq. (14), we have

$$\theta_P = \frac{\left(\frac{(\theta_N+\theta_S)}{\Delta Z^2\tau^2}N_{CR} + \frac{\pi I_a}{\sigma T_H^4} + 3\theta_{P\text{old}}^4\right)}{\left(4\theta_{P\text{old}}^3 + \frac{2N_{CR}}{\Delta Z^2\tau^2}\right)} \tag{16}$$

where N_{CR} is the Conduction–Radiation parameter $N_{CR} = \frac{k\kappa}{4\sigma T_h^3}$ and $\tau = \kappa L$. First, a temperature distribution is assumed and the radiative transfer equation [Eq. (10)] is solved to obtain new set of intensities and average intensities at each node. Eq. (16) is used to find the new non-dimensional temperatures at each node. The cycle is repeated until convergence is reached. The convergence criterion for the energy equation that has been employed here is the norm of the error between the temperatures value of any successive iteration should be less than 10^{-10}.

$$\text{Norm} = \sum_{i=1}^{n}(\theta_{i\text{new}} - \theta_{i\text{old}})^2 = 10^{-10} \tag{17}$$

4.2. Inverse problem

Before estimating the parameters of the system, we need experimental measurements from the system. However, for this study, the direct problem is solved with known parameters to obtain numerical solutions and these were used as the experimental measurements, with or without adding small random perturbations. The effect of measurement errors are taken into account with these random perturbations, as in the following equation:

$$T_{\text{measured}} = T_{\text{exact}} + \Re \tag{18}$$

where $\Re$ is a random error between ± 5.0. The perturbations are chosen such that at their highest levels, they represent an

approximately 1% error with respect to the mean temperature (450 K in this study). Once the experimental values of temperature profiles are simulated, the method proceeds under an initial assumption of some values of parameters (to be estimated) and then obtaining the temperature profile by solving the direct problem. The sum of the squares of the residuals between the estimated and measured temperatures is then obtained with Eq. (13). Genetic Algorithms is used to solve the minimization problem.

Genetic algorithms mimic the process of evaluation and hence typically work for maximization problems. Even so, the conversion of a minimization problem to maximization is straight forward as is shown below

$$F = 1/(1+R) \tag{19}$$

F is objective function of the optimization procedure and in the parlance of GA, is known as fitness function.

GA uses the values of the parameters (to be estimated) from the given range. Variables are first coded in binary strings. The length of the string is usually determined according to the desired accuracy. Thereafter, the fitness function values are calculated by substituting the variables in fitness function (Eq. (19)). After this, the population is operated upon by three main operators namely reproduction, crossover and mutation-to create a new population of points. The operation reproduction refers to the selection of the mating pool, so that "fit parents" alone produce "children". This is again done based on probabilistic rules combined with the fitness function. Crossover refers to the process of exchanging genetic material between "parents". Several types of crossover are reported in GA literature. In this study, we have employed uniform crossover, wherein the decision to exchange bits is based on the probability of crossover. This has been set to 0.5 in this study. This procedure is continued until the termination criterion is met. Details of executing an optimization with GA is available in a number of references (see for example Goldberg [7]).

5. Results and discussion

5.1. Validation and grid dependence study

The results of the present study are validated against the exact results of [8] for the case of one-dimensional radiative equilibrium between two parallel, isothermal, diffuse plates enclosing a gray isotropically scattering medium. For purposes of validation, isotropic scattering was included in the governing equations. The results are obtained for three grid sizes (4 × 10), (10 × 20) and (20 × 42) and are tabulated in Table 1. It is observed that results predicted by intermediate (10 × 20) and the fine grid (20 × 42) are in good agreement with the exact solution, and the maximum error in the fine grid is −0.036%. Therefore, for all the further calculations, a grid size of 20 × 42 is used where the number of control volume in z-direction is 20 and the number of directions is 42. Results to be presented henceforth correspond to the case of no scattering.

5.2. Forward problem

The effect of conduction–radiation parameter and emissivity on non-dimensional temperature is shown in Fig. 3a and b, respectively. Temperature profiles for the case $N_{CR} = 1$ are very similar to temperature profiles for pure conduction which are straight lines. Thus, for large values of parameter N_{CR}, the differences between temperature profiles for pure conduction and simultaneous conduction and radiation are small. However, as the parameter N_{CR} is decreased, the differences are seen to increase. Since the system under consideration is in steady state, the total heat flux, (conduction plus radiation) across the medium is constant. To ensure this, it is necessary for the variation in energy flux by conduction to be compensated by variation in the radiative fluxes. It is observed from Fig. 3b that as the wall emissivities decrease, in other words, as the boundaries become more and more reflecting, the variation of θ values increases in the vicinity of the cold surfaces. Similar trends have been observed by Viskanta and Grosh [9,10].

5.3. Inverse problem

The direct or forward problem is solved for an optical thickness $\tau = 5$, conduction–radiation parameter $N_{CR} = 1$ and emissivities of both walls $\varepsilon = 0.7$. The cold wall is at a temperature of $\theta_C = 0.5$ and the distance between the two plates $L = 1$ m. The temperature distribution obtained is taken as the "measured" temperature profile. In this

Table 1
Non-dimensional heat flux for the case of radiative equilibrium between two isothermal, diffuse, infinitely long parallel plates

Optical thickness τ	Non-dimensional heat flux $-q^* = q/\sigma\,(T_H^4 - T_C^4)$				Percentage error with respect to exact results		
	Coarse grid (4 × 10)	Intermediate grid (10 × 20)	Fine grid (20 × 42)	Exact results ([8])	(4 × 10)	(10 × 20)	(20 × 42)
0.0	1.0000	1.0000	1.00000	1.0000	0.0	0.0	0.0
0.1	0.9128	0.9145	0.91537	0.9157	−0.3	−0.13	−0.036
0.5	0.6979	0.7027	0.70384	0.7040	−0.86	−0.18	−0.023
1.0	0.5484	0.5521	0.55311	0.5532	−0.87	−0.2	−0.016
2.0	0.3874	0.3891	0.38984	0.3900	−0.67	−0.23	−0.04
5.0	0.2078	0.2074	0.20759	0.2076	0.096	−0.096	0
10.0	0.1173	0.1168	0.11678	0.1167	0.514	0.085	−0.06

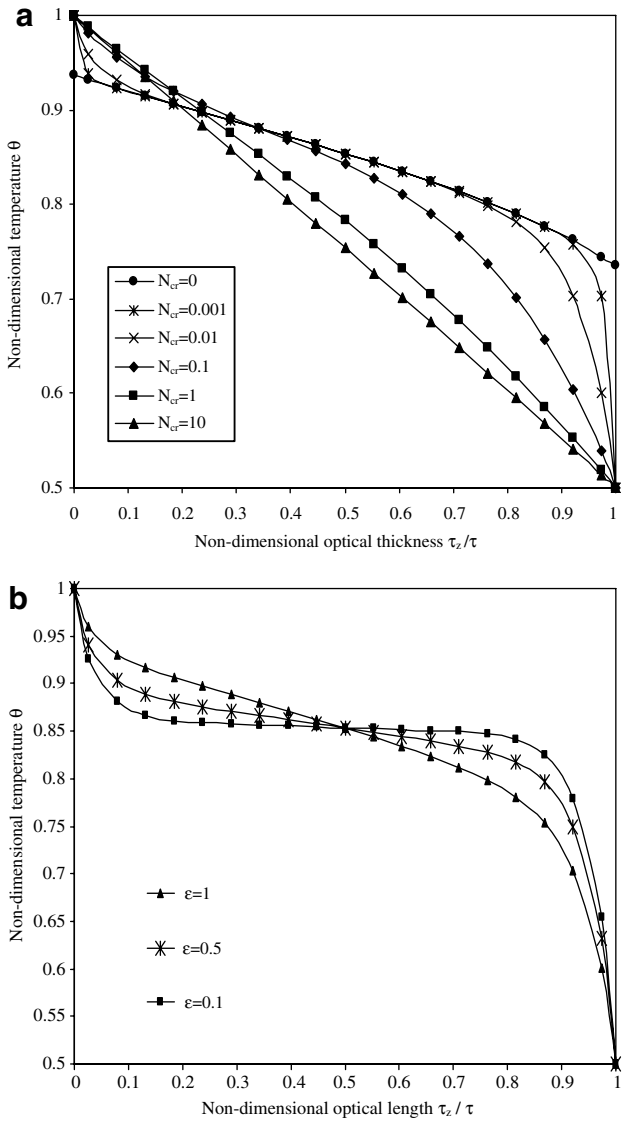

Fig. 3. (a) Variation of non-dimensional temperature θ with non-dimensional optical thickness for $\theta_C = 0.5$ and $\tau_L = 1.0$. (b) Effect on emissivity on non-dimensional temp profile for optical thickness $\tau_L = 1$, $\theta_C = T_C/T_H = 0.5$ and $N_{CR} = 0.01$.

section, we present the numerical results to demonstrate the use of genetic algorithms for the estimation of the pertinent parameters from a knowledge of the measured temperature profiles. In order to simulate the measured temperature profile with measurement errors, small random perturbations are added to the numerical solution of direct problem.

For the GA, the maximum number of generations is taken as 100. The population in each generation is also 100. The string length is 32 bits for the variable and mutation rate is 0.02.

5.3.1. Estimation of boundary emissivity ε

For estimating the boundary emissivity, the optical thickness τ and the conduction–radiation parameter N_{CR} are fixed at 5.0 and 1.0, respectively. The value of N_{CR} has been chosen on purpose so that one has comparable contributions from radiation and conduction. Minimization of the residual temperature function is done by using GA as explained before. The estimated values of wall emissivity with different values of $\Re$ are also listed in Table 2. It is observed that estimation of boundary emissivity ε (one parameter estimation) is quite accurate even with noisy data.

5.3.2. Estimation of thermal properties of medium N_{CR} and τ

In this section, the results of two parameter estimation, namely simultaneous estimation of the optical thickness τ and the conduction–radiation parameter N_{CR} is presented. Here, other parameters are kept constant at the values described in the earlier section. The results of the analysis are tabulated in Table 3 and it can be seen from the results that the accuracy in the estimation of τ is more sensitive to "measurement" errors than that of N_{CR}. The variation of residual temperature function at each generation is shown in Fig. 4. It is observed that with exact "measured" temperature profile the residual converges to value of 10^{-5} in less than 40 generations only. As the perturbation increases the

Table 2
Errors in the estimation of boundary emissivity with and without perturbation

Perturbation	True values	Estimated values	% Error
0	0.7	0.7	0
±0.01	0.7	0.699	−0.01
±0.1	0.7	0.700	0.05
±0.5	0.7	0.701	0.26
±1.0	0.7	0.703	0.52
±5.0	0.7	0.718	2.68

Table 3
Errors in the simultaneous estimation of τ and N_{CR} with and without "measurement errors" (first column indicates perturbation in temperatures in °C)

τ		N_{CR}
Actual values		
5		1
Estimated values without perturbation		
5		1
Estimated values with perturbation		
±0.01	5.0021	1
±0. 1	5.0000	1.0001
±0.5	4.9791	1.0021
±1.0	4.9602	1.0043
±5.0	4.6338	0.9795
Percent error without perturbation		
0		0
Percent error with perturbation		
±0.01	0.043	0.000
±0.1	0.000	0.010
±0.5	−0.418	0.215
±1.0	−0.795	0.431
±5.0	−7.324	2.049

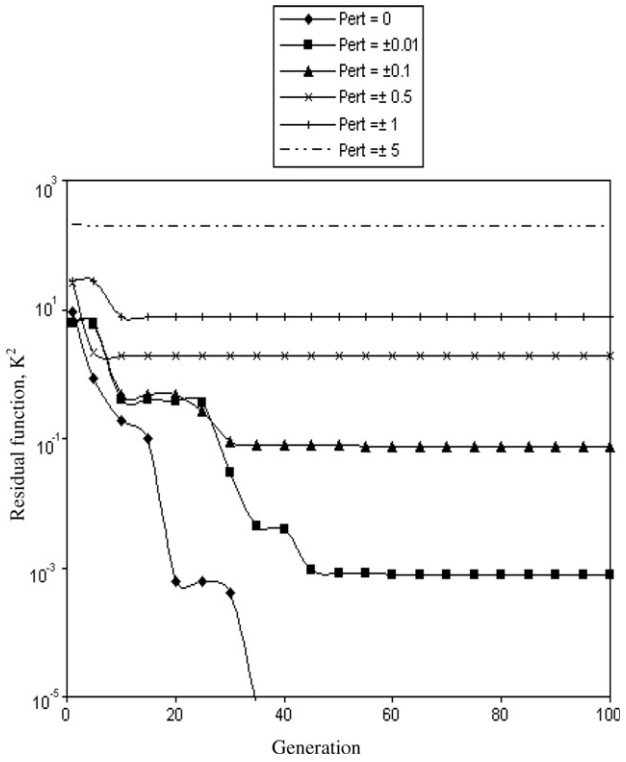

Fig. 4. Best value of the fitness function at each generation with perturbation level of 0, ±0.01, ±0.1, ±0.5, ±1.0, ±5.0.

residual value increases but there is no significant changes in the residual values after 50 generations.

5.3.3. Simultaneous estimation of properties of medium N_{CR} and τ and boundary property ε

The results for the simultaneous estimation of three parameters N_{CR}, τ and ε from the measured temperature distribution is discussed in this section. Table 4 shows the estimated values of the parameters for seven different sets of ranges. This estimation is done from the exact temperature profile obtained from numerical solution of the forward problem for $N_{CR} = 1$, $\tau = 5$ and $\varepsilon = 0.7$.

It can be seen from the results that the solution is not unique even for the exact measured temperature distribution, i.e. without perturbation of data. Different combinations of parameters are obtained for different set of range. It is observed that while constricting the range for the parameters while applying GAs for the inverse problem, we can get a combination of parameters which gives the least residual value. The average of three best runs is also given in Table 4.

Fig. 5a and b show the process of convergence of parameters for three different runs that correspond to the actual measured temperature profile. P, Q and R represent τ, N_{CR} and ε, respectively. 1, 2 and 3 correspond to three different runs. It may be seen, that for the Run3 (i.e. P3,

Table 4
Simultaneous estimation of N_{CR}, τ and ε without any perturbation

Run	Range	τ	N_{CR}	ε	Residual temp	Percentage error		
						τ	N_{CR}	ε
1	τ (0–50) ε (0–1) N_{CR} (0–15)	9.28884	3.43880	0.45413	0.14818	–	–	–
2	τ (0–15) ε (0–1) N_{CR} (0–10)	6.55848	1.71897	0.58561	0.02950	–	–	–
3	τ (1–10) ε (0.5–1) N_{CR} (0.1–3)	4.447164	0.790571	0.75196	0.00534	−11.06	−20.9	7.4
4	τ (3–6) ε (0.5–1) N_{CR} (0.5–5)	5.272892	1.112362	0.67684	0.00109	5.46	11.2	−3.31
5	τ (4.5–6) ε (0.5–0.8) N_{CR} (0.5–2)	5.95689	1.418317	0.624934	0.012815	19.3	41.8	−10.7
6	τ (4.5–5.5) ε (0.5–0.8) N_{CR} (0.5–2)	5.343597	1.142136	0.671113	0.001833	6.87	14.2	−4.12
7	τ (0.5–1.5) ε (0.6–0.75) N_{CR} (0.5–1.5)	4.914055	0.965846	0.707619	0.000113	−1.7	−3.4	1.08
Avg	–	5.1768	1.073448	0.6852	–	3.5	7.3	−2.1

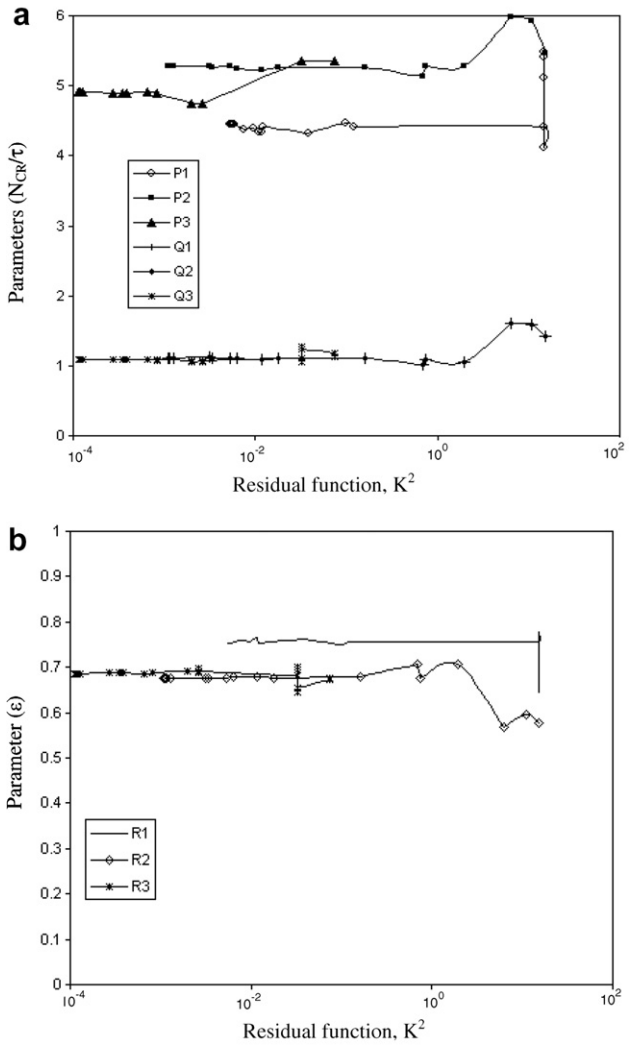

Fig. 5. (a) and (b) Simultaneous estimation of optical thickness, conduction–radiation parameter and the emissivity of wall, by inverse analysis without perturbation, P, Q and R represents τ, N_{CR} and ε, respectively, and three different runs are represented by 1, 2 and 3.

Q3 and R3), the value of the objective function is less than 1×10^{-3}. Run3 corresponds to the 7th set of data in Table 4.

Fig. 6a and b show the convergence of the parameters N_{CR}, τ, ε from the measured temperature profile for a perturbation level of ± 0.5, for three different runs. In Run1, τ varies from 0 to 50, N_{CR} varies from 0 to 15 and ε varies from 0 to 1. In Run2, τ varies from 0 to 20, N_{CR} varies from 0 to 10 and ε varies from 0 to 1 and in Run3, τ varies from 4.5 to 5.5, N_{CR} varies from 0.5 to 1.5 and ε varies from 0.6 to 0.75. In this case, different combinations of data give almost the same residual values of the temperature. More so, even after constricting the range of parameters there is no significant improvement in the objective function. Thus one can conclude that for estimation of more than two parameters by applying a simple GA, there is fat little chance of getting the estimated values, unless one has a fair idea of the range in which the parameters should lie.

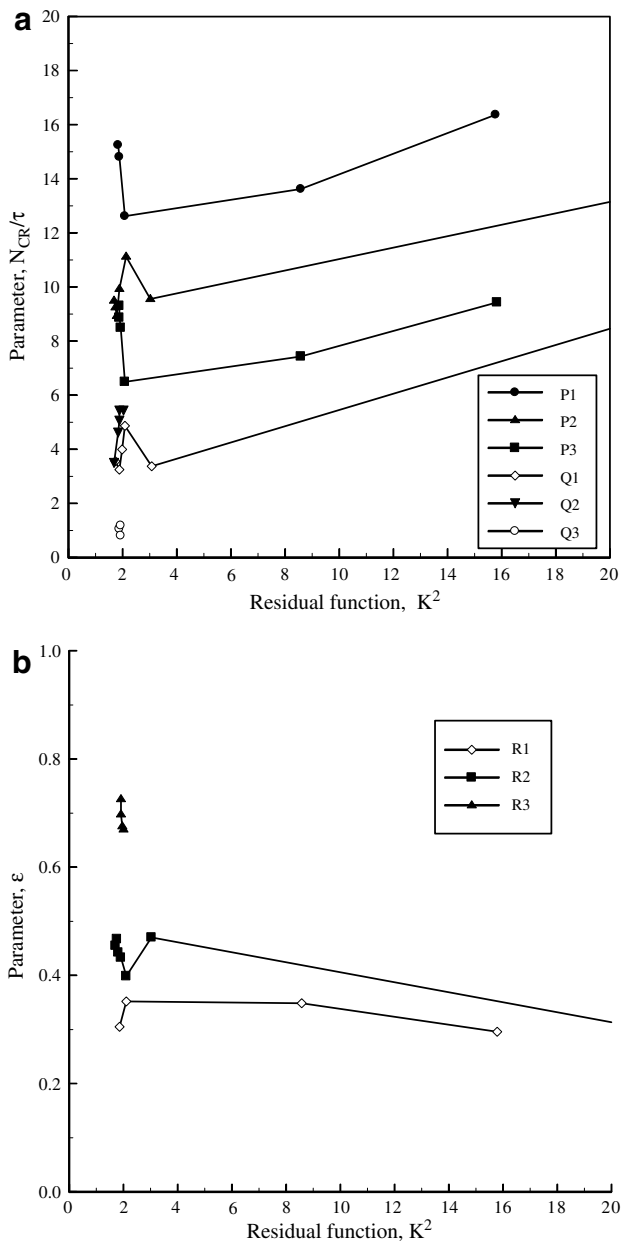

Fig. 6. (a) and (b) Simultaneous estimation of optical thickness, conduction–radiation parameter and the emissivity of wall, by inverse analysis with perturbation = ± 0.5, P, Q and R represents τ, N_{CR} and ε, respectively, and three different runs are represented by 1, 2 and 3.

For the range corresponding to Run3 mentioned above, the results for the simultaneous estimation of τ, N_{CR} and ε, with and without perturbation levels are listed in Table 5. Within this constricted range of parameters too, the percentage error with a higher perturbation level is quite appreciable.

6. Conclusions

A numerical analysis of the forward and the inverse problem is carried out in this study. The following conclusions are arrived at:

Table 5
Errors in the simultaneous estimation of N_{CR}, τ and ε within the constructed range, with "experimental errors"

	N_{CR}	τ	ε
Actual values			
	1	5	0.7
Estimated values without perturbation			
	0.9658	4.9141	0.7076
Estimated values with perturbation			
±0.1	1.032236	5.072968	0.69291
±0.5	0.910324	4.737227	0.71978
±1.0	1.187499	5.372335	0.66116
±5.0	0.950673	4.535512	0.72593
Percent error without perturbation			
	−3.42	−1.71	0.37
Percent error with perturbation			
±0.1	3.22	1.46	−1.01
±0.5	−8.96	−5.25	2.83
±1.0	18.75	7.45	−5.55
±5.0	−4.94	−9.29	3.71

(1) The existence of a thermal boundary layer near the walls is observed for the low values of N_{CR} and ε.
(2) For the "inverse problem" one parameter (ε) estimation and two parameters (N_{CR} and τ) estimation is quite accurate even with noisy data. For simultaneous estimation of N_{CR} and τ, the error in estimation of τ is more than that of N_{CR}.
(3) For simultaneous estimation of more than two parameters genetic algorithms is not very efficient unless there is a fair idea of ranges in which the parameters may lie. The solutions obtained are not always unique.
(4) In case of simultaneous estimation of N_{CR}, τ and ε without any measurement errors, nearly accurate values of the parameters are obtained by constricting the range of parameters in the search process. This reduces the value of objective function and finally more fine tuned parametric values are obtained.
(5) However, for the above mentioned case, with noisy data, the objective function values, obtained for different combinations of parameters, are almost the same. This then reduces any chances of adopting any other means to obtain more accurate solutions.
(6) For three parameter estimation, even with very constricted initial ranges of the parameters, the errors in the estimated values of the parameters are quite high whenever the input data is noisy. This is counter-intuitive as GA is generally considered to be a highly robust optimization technique.

References

[1] H.Y. Li, Estimation of thermal properties in combined conduction and radiation, Int. J. Heat Mass Transfer 40 (1999) 1545–1549.
[2] S. Manickavasagam, M.P. Menguc, Inverse radiation/conduction problem in plane parallel media, Radiat. Heat Transfer: Theory and Appl., ASME HTD 244 (1993) 67–75.
[3] N.J. Ruperti, M. Raynaud, J.F. Sacadura, A method for the solution of the coupled heat conduction–radiation problem, ASME J. Heat Transfer 118 (1996) 10–17.
[4] H.Y. Li, C.Y. Yang, A genetic algorithm for inverse radiation problems containing a participating medium, Int. J. Heat Mass Transfer 40 (1996) 1545–1549.
[5] K.W. Kim, S.W. Baek, M.Y. Kim, H.S. Ryou, Estimation of emissivities in a two-dimensional irregular geometry by inverse radiation analysis using hybrid GA, J. Quant. Spectrosc. Ra. 87 (2004) 1–14.
[6] G.D. Raithby, E.H. Chui, A finite volume method for predicting radiant heat transfer in enclosures with participating medium, ASME J. Heat Transfer 110 (1990) 415–423.
[7] David E. Goldberg, Genetic algorithm in search, Optimization and Machine Learning, Addition-Wesley Longmann Publishing Co. Inc.,, Boston, MA, 1989.
[8] M.A. Heaslet, R.F. Warming, Radiative transport and wall temperature slip in absorbing planar medium, Int. J. Heat Mass Transfer 8 (1965) 979–994.
[9] R. Viskanta, R.J. Grosh, Heat transfer by simultaneous conduction and radiation in a absorbing medium, ASME J. Heat Transfer 5 (1962) 63–72.
[10] R. Viskanta, R.J. Grosh, Effect of surface emissivity on heat transfer by simultaneous conduction and radiation, Int. J. Heat Mass Transfer 5 (1962) 729–734.